Magnetic phase transitions in TbFe2Al10, HoFe2Al10 and ErFe2Al10

Manfred Reehuis, M. W. Wolff, Alexander Krimmel, Ernst-Wilhelm Scheidt, N. Stüsser, Alois Loidl, W. Jeitschko

Angaben zur Veröffentlichung / Publication details:

Reehuis, Manfred, M. W. Wolff, Alexander Krimmel, Ernst-Wilhelm Scheidt, N. Stüsser, Alois Loidl, and W. Jeitschko. 2003. "Magnetic phase transitions in TbFe2Al10, HoFe2Al10 and ErFe2Al10." *Journal of Physics: Condensed Matter* 15 (10): 1773–82. https://doi.org/10.1088/0953-8984/15/10/323.

Magnetic phase transitions in $TbFe_2Al_{10}$, $HoFe_2Al_{10}$ and $ErFe_2Al_{10}$

M Reehuis[1,2], M W Wolff[3], A Krimmel[1], E-W Scheidt[1], N Stüsser[2], A Loidl[1] and W Jeitschko[3]

[1] Institut für Physik, Elektronische Korrelationen und Magnetismus, Universität Augsburg, D-86135 Augsburg, Germany
[2] Hahn-Meitner-Institut, Glienicker Straße 100, D-14109 Berlin, Germany
[3] Anorganisch-Chemisches Institut, Universität Münster, Wilhelm-Klemm-Straße, 8 D-48149 Münster, Germany

Abstract

The magnetic order of the orthorhombic aluminides $TbFe_2Al_{10}$, $HoFe_2Al_{10}$ and $ErFe_2Al_{10}$ (space group $Cmcm$) has been studied by specific heat and magnetic measurements, as well as by neutron powder diffraction down to 100 mK and in external fields up to 5 T. Only the rare-earth ions carry a magnetic moment. At $T = 1.5$ K the terbium moments in $TbFe_2Al_{10}$ show a square-wave modulated magnetic order with wavevector $\boldsymbol{k} = (0, 0.7977, 0)$ and a moment direction parallel to the a-axis. At a critical field of $H_{c1} = 0.9$ T one of ten spins is forced to flip, going into an intermediate ferrimagnetic phase that is stable up to the critical field $H_{c2} = 1.8$ T. Above this field finally all the rest of the spins flip, resulting in a ferromagnetic order of the terbium moments. $ErFe_2Al_{10}$ orders antiferromagnetically below $T_N = 1.77(7)$ K with a similar magnetic structure characterized by a wavevector $\boldsymbol{k} = (0, \sim 0.8, 0)$. In contrast, no signs of long range magnetic order could be observed for $HoFe_2Al_{10}$ down to 100 mK.

1. Introduction

During the last few decades a large number of aluminides $LnFe_xAl_{12-x}$ with $x = 4, 5, 6$ (Ln = lanthanide) derived from the tetragonal $ThMn_{12}$-type structure have attracted considerable attention due to their interesting magnetic properties [1–5]. Only recently, the compounds with $x = 2$ have been synthesized [6]. The magnetic order of the antiferromagnetic compounds $TbFe_2Al_{10}$ ($T_N = 16.5(5)$ K) and $DyFe_2Al_{10}$ ($T_N = 7.5(5)$ K) has been investigated by SQUID magnetometry and neutron diffraction [6, 7]. At $T = 1.5$ K the terbium sublattice shows a square-wave modulated structure with $\boldsymbol{k} = (0, 0.7977(3), 0)$, while the dysprosium moments form a helical magnetic structure with $\boldsymbol{k} = (0, 0.7836(4), 0)$. In the case of $HoFe_2Al_{10}$ and $ErFe_2Al_{10}$ no magnetic order could be detected down to 1.6 K [7]. The Pauli paramagnetism of YFe_2Al_{10} and $LaFe_2Al_{10}$ [6] and further Mössbauer measurements [8]

showed that the iron sublattice does not contribute to the observed magnetic order. This is in contrast to the aluminides $LnFe_xAl_{12-x}$ with $x = 4, 5, 6$ where both the iron and the lanthanide moments reveal long range magnetic order [1–5].

In the present work we report on the magnetization process of $TbFe_2Al_{10}$ carried out on powder samples in order to understand its metamagnetic behaviour, which has been observed only recently [6]. Further, we account for the magnetic properties of $HoFe_2Al_{10}$ and $ErFe_2Al_{10}$ down to 100 mK.

2. Experimental details

Samples of the aluminides $TbFe_2Al_{10}$, $HoFe_2Al_{10}$ and $ErFe_2Al_{10}$ were prepared in the atomic ratio Ln:Fe:Al = 1:2:12 as described earlier [6]. Starting materials were iron powder and filings of the rare-earth metals and aluminium, all with nominal purities of $\geqslant 99.9\%$. The powders were pressed into pellets and subsequently arc-melted under argon. Then the resulting buttons were annealed in evacuated silica tubes for one week at 1000 °C. The aluminium matrix was dissolved in slightly diluted sodium hydroxide and the dried powders were characterized by Guinier powder x-ray diffraction at room temperature using Cu $K\alpha_1$ radiation. Small amounts of aluminium were detected in this way.

The low temperature heat capacity of $HoFe_2Al_{10}$ and $ErFe_2Al_{10}$ has been measured on pressed pellets of about 7 mg for 250 mK $\leqslant T \leqslant$ 3 K using a standard relaxation method [9]. In the same low temperature region, the ac susceptibility has been determined for $HoFe_2Al_{10}$ and $ErFe_2Al_{10}$, complemented by dc-susceptibility SQUID measurements up to 400 K. Additionally, the field dependent magnetization of all compounds has been determined at low temperatures ($T = 1.6$ K for the holmium and erbium compounds and $T = 5$ K for the terbium compound, respectively) in fields up to 7 T employing a SQUID magnetometer (Quantum Design). The neutron powder diffraction measurements on $TbFe_2Al_{10}$, $HoFe_2Al_{10}$ and $ErFe_2Al_{10}$ were carried out on the E6 instrument at the reactor BERII of the Hahn-Meitner-Institut in Berlin. This instrument has a double focusing graphite monochromator using the reflection (002) ($\lambda = 245$ pm). In the case of $HoFe_2Al_{10}$ and $ErFe_2Al_{10}$ powder diagrams were collected at 100 mK using a dilution refrigerator. For the field dependent measurements of $TbFe_2Al_{10}$ a cryomagnet providing vertical magnetic fields up to 5 T has been used.

The nuclear and magnetic structures of the investigated compounds were refined from the powder data by standard Rietveld analyses employing the program FULLPROF [10]. The nuclear scattering lengths b(Al) = 3.449 fm, b(Fe) = 9.54 fm, b(Tb) = 7.38 fm, b(Ho) = 8.08 fm and b(Er) = 8.03 fm have been used [11]. The magnetic form factors of the ions Tb^{3+}, Ho^{3+} and Er^{3+} were taken from [12].

3. Results and discussion

3.1. The nuclear and zero-field magnetic structure of $TbFe_2Al_{10}$

The crystal structure of $TbFe_2Al_{10}$ was confirmed to be isotypic to the orthorhombic $SmFe_2Al_{10}$ (space group $Cmcm$) as refined earlier from single-crystal x-ray data [6]. For the Rietveld refinements of the data sets collected at $T = 1.5$ and 25 K we used the positional and thermal parameters of the samarium compound as starting values. The lanthanide atom Ln is on the Wyckoff position 4c(0, y, 1/4), Fe on 8d(1/4, 1/4, 0), Al(1) and Al(2) on 8g(x, y, 1/4), Al(3) and Al(4) on 8f(0, y, z) and Al(5) on 8e(x, 0, 0). Due to the relatively large number of ten positional and seven thermal parameters and the small data set containing 45 nuclear Bragg peaks the thermal parameters were not allowed to vary. An overall thermal parameter was

Table 1. The nuclear structure of $TbFe_2Al_{10}$ as obtained from the Rietveld refinements. An overall thermal parameter $B_{ov} = 0.002$ nm^2 was fixed during the refinements. The residual of the nuclear structure is defined by $R_N = \Sigma||F_o| - |F_c||/\Sigma|F_o|$ with F_o and F_c being the observed and calculated structure factors, respectively. The standard deviations in the values of the last digit are given in parentheses.

	1.5 K	25 K	295 K[a]
a (pm)	893.86(12)	893.95(11)	896.3(3)
b (pm)	1011.61(9)	1011.76(9)	1014.9(4)
c (pm)	897.91(14)	898.08(13)	901.3(3)
V (nm^3)	0.8119	0.8123	0.8199
y (Tb)	0.1256(8)	0.131(2)	—
x (Al1)	0.230(3)	0.225(4)	—
y (Al1)	0.353(3)	0.350(3)	—
x (Al2)	0.349(2)	0.345(3)	—
y (Al2)	0.137(4)	0.133(4)	—
y (Al3)	0.149(4)	0.149(4)	—
z (Al3)	0.601(3)	0.597(3)	—
y (Al4)	0.380(3)	0.381(4)	—
z (Al4)	0.043(3)	0.041(3)	—
x (Al5)	0.227(2)	0.230(3)	—
R_N	0.038(43)	0.050(43)	—

[a] The lattice constants at 295 K are taken from x-ray data [6].

fixed to $B_{ov} = 0.002$ nm^2. The results of the refinements are summarized in table 1. The refined positional parameters of the terbium compound at $T = 25$ K are in good agreement with those of the samarium compound [6], despite the moderate accuracy due to the small data set. In the case of the data set collected at $T = 1.5$ K we refined the nuclear and magnetic structures simultaneously. This allowed us to determine the parameter $y = 0.1256(8)$ of the terbium ions with a much higher accuracy. For the samarium ions in $SmFe_2Al_{10}$ the value $y = 0.1249(4)$ has been obtained at 295 K [6]. Thus, the lanthanide atoms in this structure type form layers perpendicular to the b-axis with interplanar distances very close to $b/4$.

In a previous paper we presented the magnetic structure of $TbFe_2Al_{10}$ [7]. Below the Néel temperature $T_N = 16.5(5)$ K the magnetic moments of the terbium atoms show a sine-wave modulated order. Below 11 K additional higher harmonic peaks appeared, indicating a transition into a square-wave modulated structure with $\boldsymbol{k} = (0, 0.7977(3), 0)$. The vector component k_y is very close to $4/5$ and therefore it describes a commensurate magnetic structure with the cell dimensions $a \times 5b \times c$. From the Rietveld refinements of the magnetic structure at $T = 1.5$ K a magnetic moment of $\mu_{\mathrm{exp}} = 8.33(7)\ \mu_B$ per terbium atom could be evaluated. For the nuclear and magnetic structure the residuals were $R_N = 0.030$ and $R_M = 0.083$, respectively (defined as $R_N = \Sigma||F_o| - |F_c||/\Sigma|F_o|$ with F_o and F_c being the observed and calculated structure factors and $R_M = \Sigma||I_o| - |I_c||/\Sigma|I_o|$).

In figure 1 it can be seen that the terbium atoms form zig-zag chains along the c-axis, where the interatomic distance $d_1 = 517$ pm is the shortest ($\boldsymbol{d}_1 = 2y\boldsymbol{b} - 1/2\boldsymbol{c} \approx 1/4\boldsymbol{b} - 1/2\boldsymbol{c}$). Therefore the exchange interactions via conduction electrons (RKKY) between the terbium moments may be approximately the strongest. The moments are coupled antiferromagnetically with a stacking sequence $+-+-\cdots$. The terbium atoms along the a-direction ($d_2 = 896$ pm; $\boldsymbol{d}_2 = \boldsymbol{a}$) show a parallel alignment, finally giving ferromagnetic layers which are parallel to the ac-plane and perpendicular to the wavevector $\boldsymbol{k}$. On the other hand, the adjacent zig-zag chains along the a-axis can also be considered as independent units of antiferromagnetically coupled double layers ($+-$ or $-+$). From figure 1 it becomes evident that the magnetic order within

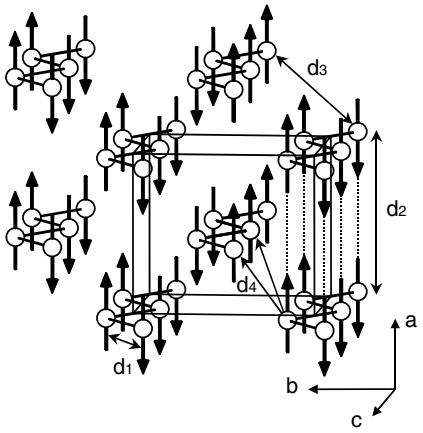

Figure 1. Orientation of the terbium moments in $TbFe_2Al_{10}$ with $\boldsymbol{k} = (0, 4/5, 0)$. The magnetic moments of the next nearest neighbour atoms forming zig-zag chains along the c-axis are coupled antiferromagnetically. Along the a-axis the moments are coupled ferromagnetically, resulting in units of antiferromagnetic double layers. The alignment between the double layers can be either parallel or antiparallel.

these double layers seems to be independent of the periodicity of the nuclear structure along the b-axis. The shortest distances of terbium atoms between these double layers are $d_3 = 677$ pm ($\boldsymbol{d}_3 = 1/2\boldsymbol{a}+1/2\boldsymbol{b}$) and $d_4 = 684$ pm ($\boldsymbol{d}_4 = 1/2\boldsymbol{a}+(1/2-2y)\boldsymbol{b}+1/2\boldsymbol{c} \approx 1/2\boldsymbol{a}+1/4\boldsymbol{b}+1/2\boldsymbol{c}$). Further, the exchange interactions of the next nearest neighbour atoms between the double layers can be ferro- or antiferromagnetic. Corresponding to the magnetic structure with $\boldsymbol{k} = (0, 4/5, 0)$ we found the stacking sequence $++--+-++--++--+-++--\cdots$ along the b-axis. It can be seen that this sequence contains units of $\cdots++--+-\cdots$. The magnetic interactions between the antiferromagnetic double layers ($+-$ or $-+$) are apparently influenced by the periodicity of the nuclear structure in such a way that a coincidence is possible when the magnetic cell has a five times larger b-axis.

3.2. Metamagnetism in $TbFe_2Al_{10}$

From the SQUID measurements of $TbFe_2Al_{10}$ carried out earlier [6], a metamagnetic transition could be observed at about 2 T. In our present work we reinvestigate the magnetization process of this compound in more detail. Figure 2 shows that a magnetic transition occurs at 1.8 T with increasing field. At 5.5 T a magnetic moment of $\mu_{\mathrm{exp}} = 6.7(2)\ \mu_B$ has finally been reached. This moment is smaller than the value $\mu_{\mathrm{exp}} = 8.33(7)\ \mu_B$ obtained from neutron diffraction data. The difference can be attributed to the fact that the magnetocrystalline anisotropy of the terbium ion is rather strong and the easy axis of magnetization (the orthorhombic a-axis) is not always parallel to the applied field for all crystallites of the powder sample. Further, it can be seen in figure 2 that the magnetization is still increasing at 5.5 T and therefore the saturation will only be reached at higher fields. In the descending field process a strong hysteresis can be observed down to 1.8 T, confirming a transition of first order. The hysteresis between 0.8 and 1.8 T is much weaker, indicating the presence of an additional intermediate ferrimagnetic phase.

In order to investigate the field induced magnetic structures in $TbFe_2Al_{10}$ we collected neutron powder patterns at the lowest attainable temperature $T = 1.6$ K and in applied magnetic fields up to 5 T. The diffraction patterns and the corresponding Rietveld refinements are shown

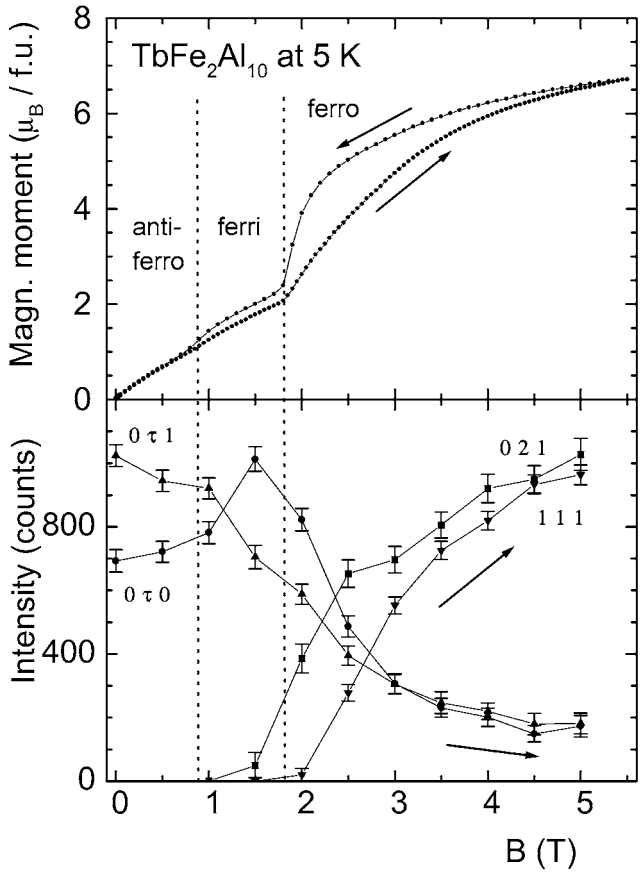

Figure 2. Field dependence of the terbium magnetic moment (upper panel) and the corresponding intensities of magnetic reflections of $TbFe_2Al_{10}$ (lower panel).

in figure 3. As described above, in zero field the magnetic moments of the terbium atoms show a square-wave modulated order with $\boldsymbol{k} = (0, 0.7977(3), 0)$ and a moment direction parallel to the a-axis. The vector component $\tau = 0.7977(3)$ is very close to 0.8 or 4/5 for a commensurate structure with a five times enlarged b-axis. From our data collected in zero field it is hard to distinguish between a commensurate and an incommensurate structure. With increasing magnetic field the magnetic peaks $(0, \tau, 0)_M$ and $(0, \tau, 1)_M$ associated with $\boldsymbol{k}$ are still observed in the range of the intermediate phase between 0.8 and 1.8 T (figures 2 and 3). But it can be seen that their intensities are strongly field dependent, indicating the presence of the intermediate ferrimagnetic phase. From our Rietveld refinements we were able to determine the magnetic structure of this phase at 1.5 T. Starting from the antiferromagnetic structure in zero field we found a stacking sequence of ferromagnetic layers along the b-axis $++--++-+--\cdots$ (figure 4). In this structure one can find ferromagnetically coupled double layers and only one single layer, which can be considered as a periodic defect. Finally, at 1.5 T our refinements revealed that just the spins of these single layers, are flipped resulting in a sequence $++--++++--\cdots$ (spin slip). This may be rationalized by the fact that a lock-in transition sets in during the magnetization process from an incommensurate to a commensurate order with $\boldsymbol{k} = (0, 4/5, 0)$. Thus, in the intermediate ferrimagnetic phase one of ten spins is

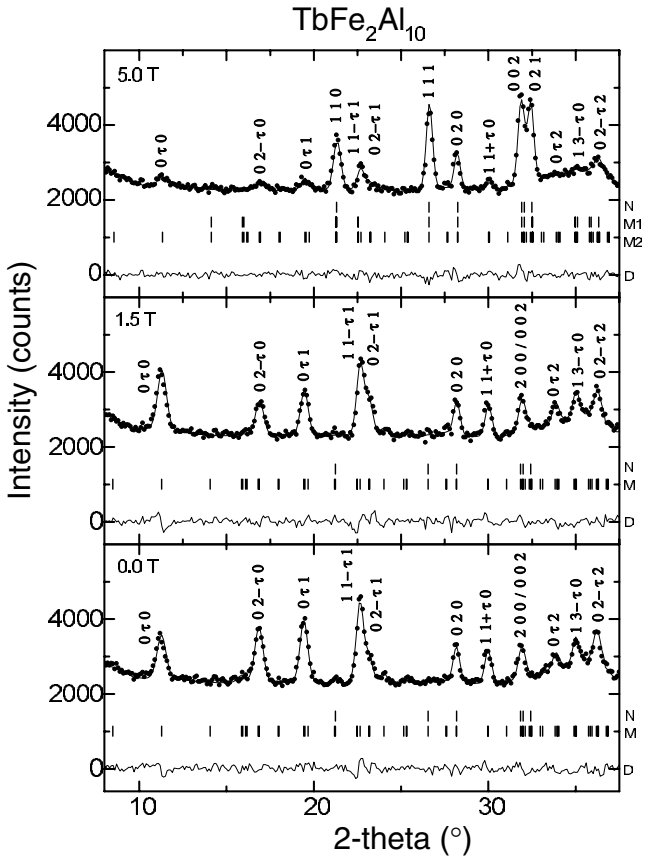

Figure 3. Rietveld refinements of the neutron powder data of $TbFe_2Al_{10}$ collected at $T = 1.6$ K and external magnetic fields of 0 T (lower panel), 1.5 T (middle panel) and 5 T (upper panel). The positions of the nuclear (N) and magnetic (M) reflections, as well as the difference between observed and calculated patterns (D), are shown.

reversed, resulting in a moment $M = 1/10\ M_0$. Spin-slip transitions have already been found in rare-earth metals like erbium [13] and other intermetallic compounds like $PrGa_2$ [14, 15].

Above the critical field $H_{c2} = 1.8$ T new magnetic peaks appeared all at positions which are allowed by the nuclear structure. Hence, the magnetic cell is the same as the orthorhombic C-centred cell. From our Rietveld refinements we could confirm a ferromagnetic order of the terbium moments with the same moment direction as observed for the incommensurate structure. Due to the presence of a vertical magnetic field a preferred orientation of the powder has been applied during the refinements. At $B = 5$ T this contribution was approximately 15%, giving residuals of $R_N = 0.047$ and $R_M = 0.080$. For the refinements of the data collected at 1.5 T it could be neglected. In fact, it is surprising that the effect of preferred orientation seems to be rather small. Here it is likely that the magnetic phase transition also sets in for crystallites where the moment direction is not strictly parallel to the vertical field. The applied vertical field may induce the phase transition without shifting the moment parallel to the field.

The incommensurate peaks decreased strongly above 1.8 T but even at 5 T these peaks had not completely disappeared. This can be ascribed to the strong anisotropy of the terbium ions as already described above. A spontaneous change as a transition of first order (spin flip) from

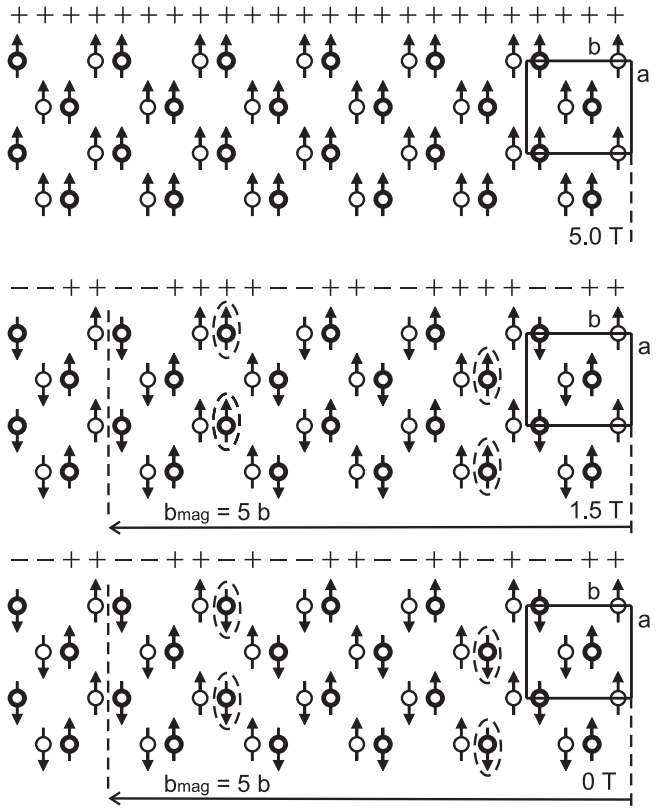

Figure 4. The magnetic order of the terbium moments in $TbFe_2Al_{10}$ at 1.6 K and magnetic fields up to 5 T. The terbium atoms in $z = 1/4$ and $3/4$ are shown as circles with thin and thick lines, respectively. In zero field the moments show an antiferromagnetic square-wave modulated structure. With increasing field up to 1.5 T two spins (enclosed by dashed ellipses) in the magnetic unit cell are forced to flip, resulting in the intermediate phase. Finally, at 5 T all the rest of the spins flip, reaching the ferromagnetic state.

the intermediate to the ferromagnetic phase should be clearly evidenced on a single crystal of $TbFe_2Al_{10}$ where the easy axis of magnetization can be perfectly aligned parallel to the applied field. Spin flip transitions were observed for many intermetallic compounds like HoAlGa [16], $TbCu_2$ [17], $PrCo_2Si_2$ [18, 19] or $DyCo_2Si_2$ [20, 21].

3.3. Magnetic properties of $HoFe_2Al_{10}$ and $ErFe_2Al_{10}$

In order to investigate the magnetic behaviour of $HoFe_2Al_{10}$ and $ErFe_2Al_{10}$ magnetic measurements have recently been performed for 1.5 K $\leqslant T \leqslant$ 300 K in fields up to 5 T [6]. However, the results did not allow for a proper characterization of the magnetic properties of $HoFe_2Al_{10}$ and $ErFe_2Al_{10}$, respectively. Whereas the experimental values of the effective paramagnetic moments ($\mu_{\rm exp}$(Ho) = 10.6(1) μ_B, $\mu_{\rm exp}$(Er) = 9.5(1) μ_B) are close to the theoretically expected ones (μ_{eff}(Ho) = 10.60 μ_B, μ_{eff}(Er) = 9.56 μ_B), the corresponding Curie–Weiss temperatures are close to zero and the susceptibilities did not reveal any indications of a well defined magnetic phase transition [6]. These measurements were re-examined in a somewhat extended field (up to 7 T) and temperature range (up to 400 K) with, however, almost identical results.

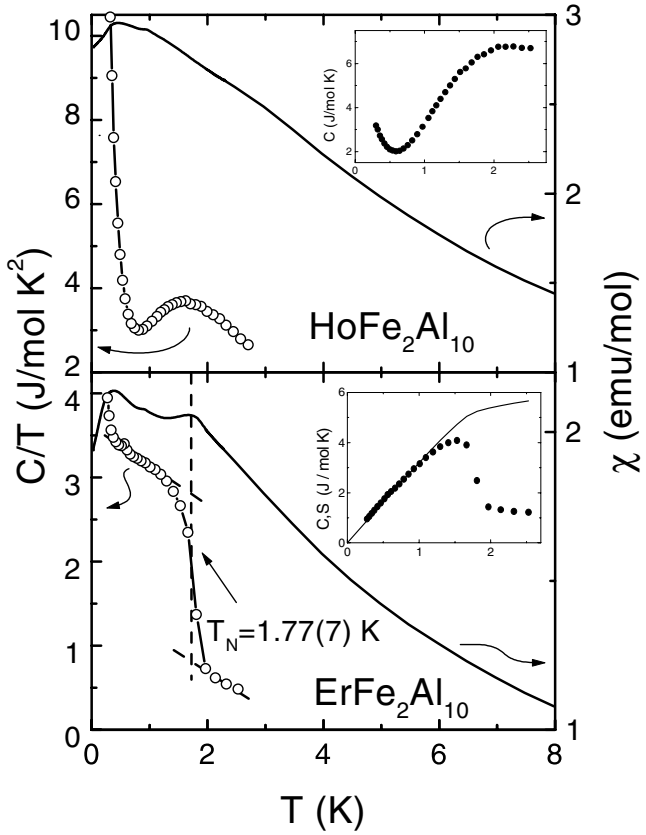

Figure 5. Low temperature specific heat $C/T(T)$ and susceptibility $\chi(T)$ of $HoFe_2Al_{10}$ (upper part) and $ErFe_2Al_{10}$ (lower part), respectively. The insets show the heat capacity $C(T)$. For Ln = Er, the corresponding magnetic entropy $S(T)$ is included in the inset (full curve).

To further elucidate the magnetic properties of $HoFe_2Al_{10}$ and $ErFe_2Al_{10}$, the specific heat and magnetic susceptibilities have subsequently been measured down to 250 mK. The results of these measurements are shown in figure 5. As evident, a well defined antiferromagnetic phase transition of $ErFe_2Al_{10}$ takes place at $T_N = 1.77(7)$ K. The corresponding entropy is obtained by integrating the specific heat data after subtraction of a small nuclear contribution and for a constant extrapolation of $C/T(T)$ towards zero. The nuclear magnetic contribution arises at low temperatures due to a Schottky anomaly of the nuclear spins and has been taken into account by a fit according to a characteristic $1/T^3$ temperature dependence for $T \leqslant 630$ mK. The entropy associated with the magnetic phase transition of $ErFe_2Al_{10}$ is very close to $R \ln 2$ (5.763 J mol^{-1} K^{-1}). The occurrence of long range antiferromagnetic order of the erbium ions could be confirmed by additional neutron powder diffraction experiments at very low temperatures. In the neutron powder patterns collected at 100 mK we could observe magnetic reflections. Here it has to be mentioned that the signal-to-noise ratio was rather poor, partly because of the strong thermal neutron absorption cross section of erbium. Therefore, the magnetic structure could not be determined unambiguously. In the difference pattern I ($T = 100$ mK) − I ($T = 3$ K) shown in figure 6, magnetic peaks could be observed which are associated with a wavevector $\boldsymbol{k} = (0, \sim 0.8, 0)$, as found for the terbium and dysprosium

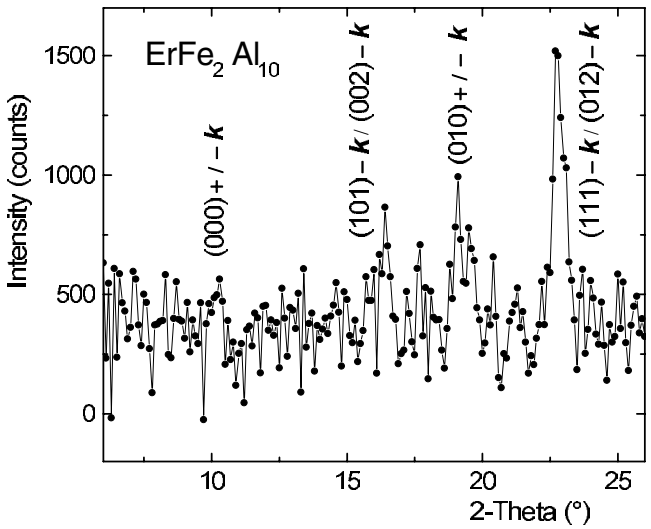

Figure 6. Difference pattern of $ErFe_2Al_{10}$ obtained from the powder diffraction patterns at 100 mK and 3 K.

compounds. The strongest magnetic intensity is found at the positions of the overlapping peaks $(111)^-$ and $(012)^-$ at about $2\theta \approx 23°$. In contrast, the expected principal magnetic reflection $(000)^{\pm}$ seems to be absent. Only when the erbium moments show a sine- (or square-) wave modulated order with a moment direction parallel to $\boldsymbol{k}$ is the corresponding magnetic intensity expected to be zero. It is calculated to be relatively weak when a helical order is assumed, where the moments rotate within the ab-plane. It is interesting to note that both structures are different to those of $TbFe_2Al_{10}$ and $DyFe_2Al_{10}$, respectively. The estimated ordered magnetic moment per erbium ion is about 7 μ_B.

The upper part of figure 5 shows the low temperature susceptibility and specific heat for $HoFe_2Al_{10}$. These data do not provide any evidence for a magnetic phase transition above $T \geqslant 250$ mK. It can be seen from figure 5 that the holmium compound shows a maximum of the C/T-values at about 1.5 K that can be ascribed to a Schottky anomaly with a corresponding energy gap of $\Delta \approx 3$ K. Small exchange interactions between the holmium ions and the presence of a CEF singlet ground state do not allow for any long range magnetic order down to very low temperatures. This is confirmed by our neutron diffraction study, where no magnetic intensities were detected down to 100 mK.

The Néel temperatures show a strong decrease from the terbium to the erbium compound. No agreement can be found when the values are compared to the de Gennes function $T_N \propto (g-1)^2 J(J+1)$ [22] where g is the Landé factor and J the total angular momentum of the Ln^{3+} Hund's rule ground state. For $DyFe_2Al_{10}$ a Néel temperature of 11.1 K is expected instead of $T_N = 7.5$ K. For $HoFe_2Al_{10}$, the de Gennes ordering temperature is calculated to be 7.1 K, but no magnetic order could be found down to 100 mK. It is further interesting to see that $ErFe_2Al_{10}$ again shows an antiferromagnetic order below $T_N = 1.77$ K, compared to the expected transition temperature according to the de Gennes scaling of 4.0 K. It seems obvious that the de Gennes function cannot be used for intermetallic compounds with very low lanthanide content. In the currently investigated aluminides the magnetic order seems to be mainly influenced by the single-ion anisotropy, which is usually very strong in terbium compounds. An unusual, but different behaviour could already be found in the ternary

phosphides $Ln_2Ni_{12}P_7$ (Ln = Tb, Dy, Ho, Er) where the content of lanthanide atoms is also low. There, the magnetic order of the Tb, Dy and Ho sublattices sets in at around 10 K, whereas no magnetic order could be detected for the Er atoms down to 1.6 K [23, 24].

Acknowledgments

We thank S Kausche and Dr P Smeibidl for technical support during the neutron diffraction experiments. This work has been supported by the BMBF under contract number 13N6917-A/Elektronische Korrelationen und Magnetismus.

References

[1] Buschow K H J and van der Kraan A M 1978 *J. Phys. F: Met. Phys.* **8** 921
[2] Bargouth M O, Will G and Buschow K H J 1977 *J. Magn. Magn. Mater.* **6** 129
[3] Felner I and Nowik I 1978 *J. Phys. Chem. Solids* **39** 951
[4] Kockelmann W, Schäfer W, Will G, Fischer P and Gal J 1994 *J. Alloys Compounds* **207/208** 311
[5] Felner I, Seh M, Rakavy M and Nowik I 1981 *J. Phys. Chem. Solids* **42** 369
[6] Thiede V T, Ebel T and Jeitschko W 1998 *J. Mater. Chem.* **8** 125
[7] Reehuis M, Fehrmann B, Wolff M W, Jeitschko W and Hofmann M 2000 *Physica* B **276–278** 594
[8] Ebel T 1995 *Doctoral Thesis* Universität Münster
[9] Bachmann R, DiSalvo F J Jr, Geballe T H, Greene R L, Howard R E, King C N, Hirsch H C, Lee K N, Schwall R E, Thomas H-U and Zubeck R B 1972 *Rev. Sci. Instrum.* **43** 205
[10] Rodriguez-Carvajal J 1993 *Physica* B **192** 55
[11] Sears V F 1992 *International Tables for Crystallography* vol C, ed A J C Wilson (Dordrecht: Kluwer Academic) p 383
[12] Brown P J 1992 *International Tables for Crystallography* vol C, ed A J C Wilson (Dordrecht: Kluwer Academic) p 391
[13] Gibbs D, Bohr J, Axe J D, Moncton D E and D'Amico K L 1986 *Phys. Rev.* B **34** 8182
[14] Ball A R, Gignoux D and Schmitt D 1993 *J. Magn. Magn. Mater.* **130** 317
[15] Gignoux D and Schmitt D 1995 *J. Alloys Compounds* **225** 423
[16] Ball A R, Gignoux D, Schmitt D, Zhang F Y and Reehuis M 1992 *J. Magn. Magn. Mater.* **110** 343
[17] Iwata N, Kimura T, Shigeoka T and Hashimoto Y 1987 *J. Magn. Magn. Mater.* **70** 279
[18] Shigeoka T, Iwata N, Fujii H, Okamoto T and Hashimoto Y 1987 *J. Magn. Magn. Mater.* **70** 239
[19] Shigeoka T, Fujii H, Yonenobu K, Sugiyama K and Date M 1989 *J. Phys. Soc. Japan* **58** 394
[20] Iwata N, Honda K, Shigeoka T, Hashimoto Y and Fujii H 1990 *J. Magn. Magn. Mater.* **90/91** 63
[21] Shigeoka T, Garnier A, Gignoux D, Schmitt D, Zhang F Y and Burlet P 1994 *J. Phys. Soc. Japan* **63** 2731
[22] de Gennes P G 1958 *C. R. Acad. Sci., Paris* **247** 1836
[23] Zeppenfeld K and Jeitschko W 1993 *J. Phys. Chem. Solids* **54** 1527
[24] Reehuis M, Krimmel A, Ebel T, Jeitschko W and Loidl A 2003 to be published